Analyst

A Linear Mass Concentration Detector for Solvent Gradient Polymer Separations

Journal:	*Analyst*
Manuscript ID	AN-ART-12-2019-002533.R1
Article Type:	Paper
Date Submitted by the Author:	30-Mar-2020

Complete List of Authors:	Mordan, Emily; University of Michigan, Department of Chemistry Wade, James; Dow Chemical, Analytical Science, Core R&D; Pearce, Eric; Dow Chemical, Analytical Science, Core R&D Meunier, David; The Dow Chemical Company, Core R&D Bailey, Ryan; University of Michigan, Department of Chemistry

A Linear Mass Concentration Detector for Solvent Gradient Polymer Separations

Emily H. Mordan,[1] James H. Wade,[2] Eric Pearce,[2] David M. Meunier,[2]* and Ryan C. Bailey[1]*

[1]*Department of Chemistry, University of Michigan, Ann Arbor, MI 48109 United States*

[2]*Core R&D Analytical Sciences, The Dow Chemical Company, Midland, MI 48667, Unites States*

* *ryancb@umich.edu and DMMeunier@dow.com*

Abstract

Characterization of copolymers requires the measurement of two distributions—molecular weight (MW) and chemical composition (CC). Molecular weight distributions (MWD) are traditionally determined using size exclusion chromatography (SEC) run under isocratic solvent conditions. Chemical composition distributions (CCD) are often determined using liquid adsorption chromatography (LC) with solvent gradients. The use of solvent gradients, however, often limits options of compatible detectors. A gradient compatible, universal linear mass concentration detector is a longstanding unmet need. Many industrially-relevant polymers lack chromophores or other discriminating moieties requiring detectors with a universal response. Differential refractive index (dRI) is incompatible with gradient elution due to its small dynamic range. Charged aerosol detectors (CAD) and evaporative light scattering detectors (ELSD) are probably the most promising options for gradient elution detection, but both suffer from a nonlinear mass concentration response. Silicon photonic microring resonators are optical sensors that are responsive to changes in the local refractive index (RI). The substantial dynamic range of this technology makes it attractive for refractive index-based detection during solvent gradient elution. Previously, the microring resonator platform was used as a SEC detector to characterize the MWD of broadly dispersed polystyrene (PS) standards. In this study, we demonstrate the gradient compatibility of the microring resonator platform for polymer detection by quantifying the CCD of polymer blend components. Control experiments were run with UV and ELSD detection, highlighting the uniqueness of the platform as a linear mass concentration detector with a universal detector response.

Introduction

Characterizing polymeric samples by size, composition, structure, and purity can help solve many challenges in industrial polymer manufacturing. Comprehensive characterization of polymers requires a suite of analytical methods with the ultimate goal of establishing structure property relationships.[1] Continuing advances in polymer chemistry and advanced manufacturing have enabled commercial viability of increasingly complex polymer systems. This complexity demands continued advances in polymer characterization methods.[2] For instance, homopolymers such as polystyrene or high density polyethylene can be well characterized by molecular weight distributions (MWD).[1] The standard bearer for MWD determination is size exclusion chromatography (SEC) coupled to a UV/Visible (UV) or differential refractometer (dRI) for linear mass concentration detection.[3,4,5]

Nearly all modern product development in the polymer industry involves copolymer commercialization because of the need for a balance of properties in most new materials. Polymers with two or more incorporated monomers leads to an inherent chemical composition distribution (CCD). Much like MWD, CCD dictates many physical properties of polymers including melt temperature, thermal stability, solubility, and mechanical properties such as tensile strength.[1,6] As such, CCD measurements are a vital component of copolymer characterization.

Traditional techniques for characterizing chemical composition (CC) of copolymers include mass spectrometry (MS), various spectroscopic methods, and liquid chromatography (LC). MS and spectroscopic methods (e.g., NMR, FT-IR) provide an averaged measure of CC rather than a distribution. Given that copolymers are heterogeneous in both CC and MW, a compositional average does not provide the most comprehensive characterization.[7] More informative distribution measurements require a separation of polymer components. Therefore, CC characterizations by MS or NMR often use preparative fractions obtained by SEC or LC, or these techniques are often hyphenated directly in-line with these separations methods.[8,9,10,11,12] However, the complexity of these hyphenated techniques is such that gradient elution high performance liquid chromatography (HPLC) has emerged as the most commonly used approach for CCD measurements in practice.[13]

Gradient elution LC achieves separations based on CC and functions by increasing the elution strength of the mobile phase throughout the experiment. Analytes with a high affinity for the stationary phase adsorb onto the column and are eluted once there is a higher affinity for the mobile phase.[14] The challenge, however, with gradient LC is a lack of available/compatible detectors.

The most common options for GPC characterization of polymers include dRI, UV, charged aerosol detectors (CAD)[,4,15,16], and evaporative light scattering detectors (ELSD);[17,18,19,20] however, each of these has limitations for certain applications. dRI lacks the dynamic range to track the gradient baseline and obviously any analytes eluting during the gradient. UV detectors, widely used in gradient LC, give linear mass concentration response, but many industrial polymers, including polyolefins, polyacrylates, and polyalkoxides lack chromophores.[21] Because of their universal response, CAD and ELSD are preferred as gradient compatible detectors for polymer analysis. Both CAD and ELSD nebulize and evaporate off the mobile phase prior to detection, but they give a non-linear response as a function of polymer concentration and solvent composition. This non-linearity is a major limitation of both CAD and ELSD for industrial polymer CCD as it substantially complicates quantitative measurements.[20,22, 23] It is important to mention that one approach to overcoming ELSD non-linearity is actually linearizing the response. This is often done by applying a correction to the ELSD signal and has been shown to give good correlation with isocratic GPC data compared to traditional detectors.[24]

Silicon photonic microring resonators are a type of whispering gallery mode optical sensor that detects small changes in refractive index (RI) at the sensor surface.[25] The microring resonator platform offers a very large RI dynamic range making the sensor gradient compatible, as has been previously demonstrated.[26] This is in contrast to conventional dRI detectors, which are not gradient compatible because of their small dynamic range. As a result, dRI detectors can only be used for CCD type measurements as a concentration detector for an isocratic dimension in concert with multidimensional separations.[27]

Typically, the microring resonator platform is implemented as a biosensor for monitoring molecular binding events on the sensor surface.[25,28,29,30] Much work has also been done interfacing similar optical resonator detectors with various separation methods such as gas chromatography[31] and capillary electrophoresis,[32,33,34] and recently a microwave interferometer was interfaced with HPLC for gradient separations.[35] In addition, our previous work demonstrated the applicability of microring resonator platform for industrial polymer analysis. Here we interfaced SEC separations with the microring resonators to determine the MWD of broad range polystyrene (PS) standards. These experiments were performed in conjunction with separate dRI and UV experiments to demonstrate the agreement of MWD determined by the microrings to these conventional detectors.[36]

Herein, we demonstrate the quantification of CC by utilizing the microring resonator platform as a RI based gradient elution detector. Using poly(styrene-co-methyl methacrylate) (PS-PMMA) copolymer standards, the microring resonator platform was calibrated for polystyrene (PS)/polymethacrylate (PMMA) composition. The mass linearity of the microring resonators was demonstrated and directly compared to identical experiments performed with UV and ELSD detection. Additionally, copolymer blends were created using the same PS-PMMA standards and these blends were analyzed using all three detection methods. The composition calibration allowed for identification of blend components, while mass calibrations allowed for quantification of the abundance of each component. These results demonstrate the versatility and applicability of the microring resonator platform for characterizing industrial polymers with a single detector.

Experimental

Materials

High purity solvents were all purchased from Sigma-Aldrich (St. Louis, MO). Poly(styrene-co-methyl methacrylate) (PS-PMMA) standards were purchased from Polymer Source, Inc. (Dorval, QC). Polystyrene (PS) and polymethacrylate (PMMA) homopolymer standards were purchased from Agilent (Santa Clara, CA). All polymer standards were used as received. Four 10 mg/mL PS-PMMA standards varying in PS content (82%, 54%, 31%, and 14% mol PS, provided by vendor) were prepared in chloroform and two 10 mg/mL homopolymer samples (70kDa PS and 70kDa PMMA) were prepared in chloroform.

Microring Resonators

The microring resonator system (Maverick M1 optical scanning instrumentation) and sensor array chips were purchased from Genalyte, Inc. (San Diego, CA). Detailed descriptions of sensor fabrication and instrument operation has been described elsewhere.[26]

Microring resonators are ring-shaped optical cavities of 30 µm diameter with adjacent linear waveguides. 128 individually addressable microring sensors are arranged in an array on a 4 mm x 6 mm chip. Sensor chips have a protective photoresist coating that is removed before use by successively immersing chips in acetone and isopropanol baths, followed by an acetone rinse.

Each individual microring is probed by an external tunable cavity diode laser centered at 1550 nm. Optical transmission is monitored as a function of wavelength, and dips in transmittance signal occur at resonant wavelengths defined by the following equation.

$$\lambda_r = \frac{2\pi r n_{eff}}{m} \quad (1)$$

where r is the ring radius, n_{eff} is the effective refractive index, and m is a constant. As the refractive index environment surrounding the sensor surface changes, such as analyte elution or a switching mobile phase composition, the resonant wavelength will shift. These changes in resonance wavelengths correspond to changes in n_{eff} which are monitored as a function of time and referred to as relative shift in units of delta picometers (Δpm).[37,25]

Table 1: Gradient HPLC Method

	Time (min)	Mobile Phase	
		95:5 Cyclohexane:THF	THF
Starting Condition	0	95%	5%
Isocratic hold	10.5	95%	5%
Gradient time	30.5	10%	90%
Purging	40.5	10%	90%
Re-conditioning	60.5	95%	5%

HPLC

Chromatographic separations were performed on a Waters Alliance e2695 separation module (Milford, MA) equipped with a Waters 2489 UV/Visible detector and a Waters 2424 ELSD detector. A Kromasil (Bohus, Sweden) column was used for all separations. Column dimensions were 250 mm X 4.6 mm and the packing material was 5 µm silica particles with 60 Å pores.[20,38,39,40] A 0.4 mL/min flow rate was maintained for a gradient of 95% cyclohexane (spiked with 5% tetrahydrofuran (THF)) to 90% THF (Table 1) and the column oven was held at 35°C. To increase mass on the column, multiple 5 µL injections of polymer were injected in isocratic mode using initial gradient conditions.[41,42] This method was utilized to maintain small injections and prevent polymer breakthrough.[43] The Waters 2489 UV/Visible detector wavelength was set to 260 nm with a sampling frequency of 10 HZ. The Waters 2424 ELSD detector operated at a gain of 20, gas pressure of 20 psi, drift tube temperature of 50°C, and a nebulizer temperature of 12°C.

HPLC-Microring Resonator Interface

The microring resonator cartridge was assembled by placing the sensor chip on an anodized aluminum cartridge base followed by a polyethylene terephthalate (Mylar) gasket and a polytetrafluoroethylene (Teflon) cartridge top. The Mylar gasket and Teflon cartridge top direct fluid flow across the chip and the whole assembly is secured together by screws. 1/16" PEEK tubing with a 0.25 mm flangeless ¼-28 interface were used to couple the HPLC directly to the microring resonator cartridge, as described previously.[36] For a diagram of the cartridge assembly see Figure S1 of the Supporting Information.

Once assembled the cartridge can be handled much like a flow cell, with a volume of approximately 2 µL, requiring no further handling of the sensor chip. Additionally the chip which is composed of silicon dioxide is robust enough to be used repeatedly without degraded sensor performance. Fouling is often an issue with surface based sensors especially with biological applications, however that is not an area of concern here since with LC methods analytes only come in contact with the sensor chip once they are in favorable solvents which mitigate any affinity they might have for the surface.

Data Analysis

Data analysis was carried out using custom software written in R (version 3.4.1) and RStudio (version 1.0153). Chromatograms were obtained for all the detection methods by plotting signal intensity as a function of time. Microring resonator data was obtained for each individual ring and individual ring responses were averaged to obtain the averaged response. This averaged raw data was then baseline corrected to account for the sloping baseline resulting from the continually changing mobile phase composition (Figure 1). The sloping baseline spans over a relative shift exceeding 800 ∆pm, therefore peaks on a scale of 2-15 ∆pm are initially obscured by the background baseline and overlapping traces (see Figure 1A-B). Peaks begin to become slightly visible by zooming in on the raw chromatogram, dashed lines are used to guide eye of peak location, (Figure 1B) but this is still not sufficient for any useful identification or quantification. An alternative plot of Figure 1B is presented with Figure S2, which allows for better visibility of peaks before correction. Baseline correction was necessary to remove the background baseline caused by the solvent gradient. Baseline correction was performed by fitting the sloping gradient observed in Figure 1B to a third order polynomial and subtracting the fit from the raw data (seen in Figure 1C). The resultant chromatogram was smoothed with a locally estimated scatterplot smoothing function (LOESS), a common smoothing function for time series data.[44] The final corrected microring resonator chromatogram resembles chromatograms obtained by more traditional detectors, as shown in Figure 1D. All chromatographic calculations were performed on baseline corrected and smoothed data. Lastly, this baseline correction process is very robust since identical gradient methods will always observe the same RI change since this is a function of mobile phase, therefore baseline response is very reproducible making correction for this routine.

Results and Discussion

Gradient Separation of PS-PMMA Copolymers

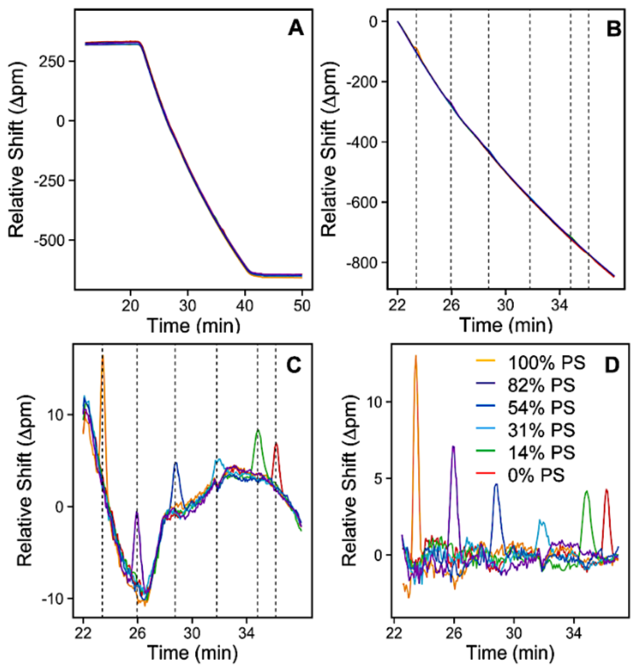

Figure 1: Data Treatment Process for Microring Resonators
A. Raw overlapping microring traces shows direct monitoring of gradient mixing though experiment since RI changes with changing mobile phase, this means gradient shape/slope is very reproducible for identical methods. **B.** A subset of **A** shows small peaks can be observed on the sloping baseline (peak location is indicated by dashed lines). This sloping baseline is fit to a third order polynomial which is then used to baseline correct the data. **C.** The fit obtained from the baseline observed in B is extrapolated and subtracted from the raw data. **D.** Then finally the subtracted chromatogram can be further corrected by applying a LOESS function.

The described gradient method outlined in Table 1 was applied to 0.15 mg injections of PS-PMMA copolymer samples prepared in chloroform, and varying in PS content covering the full range of 100%-0% moles PS (0% - 100% moles PMMA). Peaks begin to elute from the column with increasing THF content, with 100% PS eluting the earliest in the gradient given that it is the least polar. Therefore, elution order is highest to lowest PS content (lowest to highest PMMA content), with the 100% PMMA standard taking the longest to elute from the column. Detection of the described separation was implemented using three detection methods; microring resonators (Figure 2A), ELSD (Figure 2B) and UV (Figure 2C). UV and microring resonators were connected in series, ELSD data was obtained in a separate experiment due to the destructive nature of the detection technique. A chart of the used flow path can be found in Figure S3 of the Supporting Information.

A comparison of the UV, ELSD, and microring resonator detectors is shown in Figure 2. The most notable difference between the ELSD and microring resonator detectors is increased noise of the microring resonator chromatograms, where the average signal to noise ratio of the microrings is approximately 4 orders

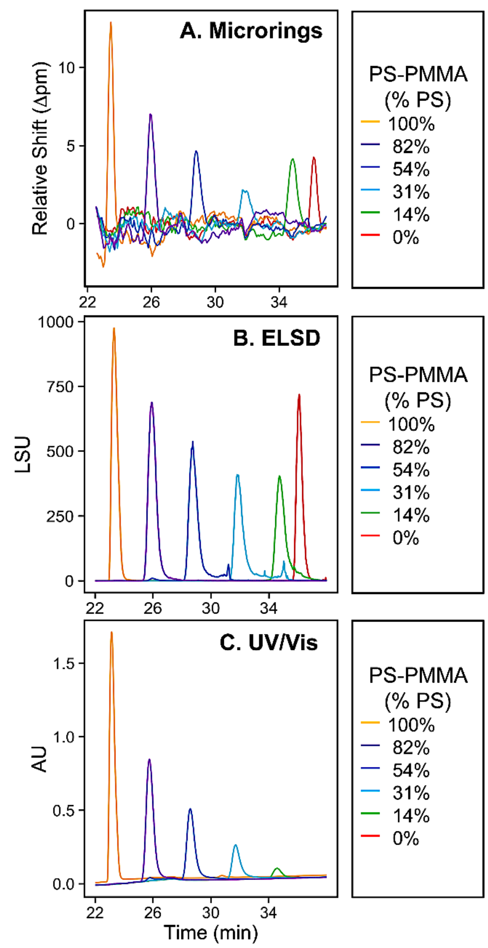

Figure 2: Gradient LC Chromatogram Comparison Separations of PS-PMMA copolymers with a cyclohexane to THF gradient. Samples were prepared in chloroform at a concentration of 10 mg/mL and a mass of 0.15 mg was injected. Chromatograms were obtained by all three detectors **A.** microring resonator platform, **B.** Evaporative light scattering (ELSD), and **C.** UV/visible (UV).

of magnitude smaller than UV and ELSD. This increased level of noise was somewhat expected since the microring resonator platform is held under ambient conditions susceptible to temperature fluctuations, whereas the UV and ELSD detectors are far less sensitive to temperature variations. The impact of temperature on the microring resonator signal has been discussed elsewhere, however, it is estimated that a 0.1°C change in temperature results in ~4.5 Δpm change in microring resonator response (this estimate was determined in a related study).[36,26]

Other comparisons that can be made are the differences of peak heights observed as the PS content changes. For the microring resonators (Figure 2A) this decrease in peak height is due to the changing RI contrast as PMMA content is increased. The respective RI (*n*) of PS, PMMA, cyclohexane and THF are as follows; 1.59,[45] 1.49,[46] 1.43, and 1.41, at 20 °C and 632.8 nm. The 31% PS-PMMA peak provided the smallest response from the microring resonators. This is caused by a combination of the RI contrast and the decreased sensitivity of the microring resonator platform for high molecular weights. With increasing molecular weight, the radius of gyration of a random polymer coil in solution also increases, and polymers with larger radiuses of gyration have portions that extend beyond the evanescent field of the sensor causing this sensitivity fall-off. This molecular weight dependence has been investigated and described previously.[36,47] All PS-PMMA standards have a molecular weight within a range of 60-80 kDa, with the exception of 31% PS which has a molecular weight of 117 kDa. These were available choices at the time of purchase. As for the changing peak heights with the ELSD chromatogram (Figure 2B) this is most likely due to scattering differences as shape and size of analyte particle varies with different PS:PMMA ratios and elution solvent composition. Finally, for the UV chromatogram (Figure 2C) there is a consistent decrease in peak height as PMMA content is increased, corresponding to the decrease in the UV-active PS component. These visual observations of peak height/area are further supported by a more quantitative comparison of peak integrations for the three detectors' chromatograms (Figure S4).

Verification of Interface Integrity

Retention times were obtained from chromatograms of all three detection methods (microring resonators, ELSD, and UV) and representative chromatograms are presented in Figure 2. This was used to calibrate for copolymer composition, the % moles of PS were plotted against the PS/PMMA peak elution time for each polymer composition standard, as shown in Figure 3. Data points represent the average retention times for three replicated experiments (n=3). There is very little variance among individual retention times so error bars are small, this verifies interface robustness. Overlaying all three calibrations on the same axis highlights indistinguishable slopes attributed by the agreement across detectors and lack of significant dead volume in the flow path. The fitting parameters of these curves can be found in Table 2. Additionally, these compositional calibrations can be useful for the identification of unknown PS-PMMA samples or blend samples that have multiple components or for computing the chemical composition distribution of a broad PS-PMMA copolymer of unkown composition.

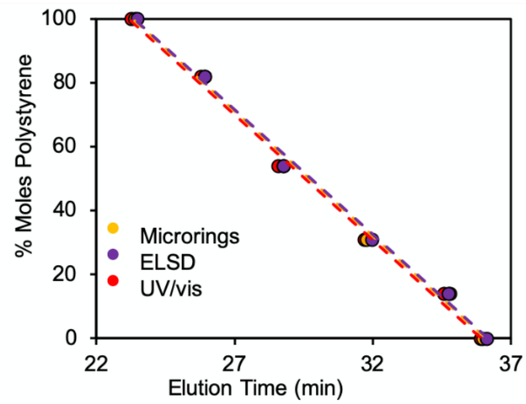

Figure 3: Copolymer composition versus elution times. Elution times from the chromatograms obtained in Figure 1 were plotted against % moles of polystyrene for each copolymer. Resulting in calibrations for copolymer composition. Plotting all three calibrations on the same axis show overlapping curves, verifying interface integrity such as no dead volume or delay between detectors.

Table 2: Fitting Parameters for Polystyrene Content Calibration

	Detector	b *x* + c		R^2
		b	c	
A	Microrings	-7.830	281.4	0.9954
B	ELSD	-7.834	283.1	0.9962
C	UV/vis	-7.829	282.5	0.9947

Mass Concentration Response Curves

Using the same PS-PMMA copolymer samples prepared in chloroform and the same experimental method discussed earlier, gradient separations were performed for various injected masses ranging from 0.15 to 0.75 mg for each detector.

Table 3: Linear Fitting Parameters for Mass Detection

	Detector	Standard (%PS)	b x + 0	R^2
			b	
A	Microrings	100	36.10	0.9819
		82	33.25	0.9848
		54	29.53	0.9924
		31	23.66	0.9585
B	UV/vis	100	221.4	0.9942
		82	211.2	0.9621
		54	148.6	0.9971
		31	73.68	0.9727

Table 4: ELSD Fitting Parameters for Mass Detection

	Detector	Standard (%PS)	b x^2 + c x + 0		R^2
			b	c	
C	ELSD	100	38.35	110.3	0.9996
		82	30.07	131.1	0.9953
		54	72.11	73.34	0.9961
		31	29.35	92.81	0.9921

Table 5: LOD and LOQ Comparison

	Detector	Standard (%PS)	LOD (µg)	LOQ (µg)
A	Microrings	100	220	550
		82	240	590
		54	270	670
		31	340	840
B	UV	100	0.0055	0.011
		82	0.0057	0.011
		54	0.0082	0.016
		31	0.016	0.032
C	ELSD	100	0.0017	0.0043
		82	0.0015	0.0036
		54	0.0026	0.0065
		31	0.0021	0.0051

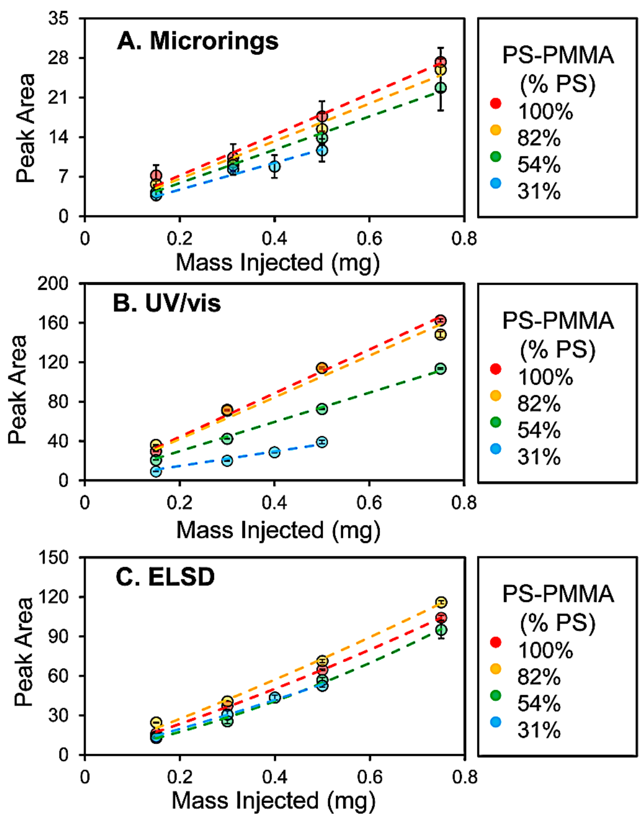

Figure 4: Mass Detection Calibrations A. Repeating cyclohexane:THF gradient separations of PS-PMMA copolymers at 4 different injected masses for 4 standards demonstrated the linearity of the microring resonators. Plotting mass injected against peak area illustrates this linear correlation. **B.** Comparable linear correlation is also observed by UV/visible (UV) detection. **C.** However plotting mass injected against peak area for evaporative light scattering (ELSD) demonstrates the non-linearity of the detector. (Mass Range: 0.15-0.75 mg)

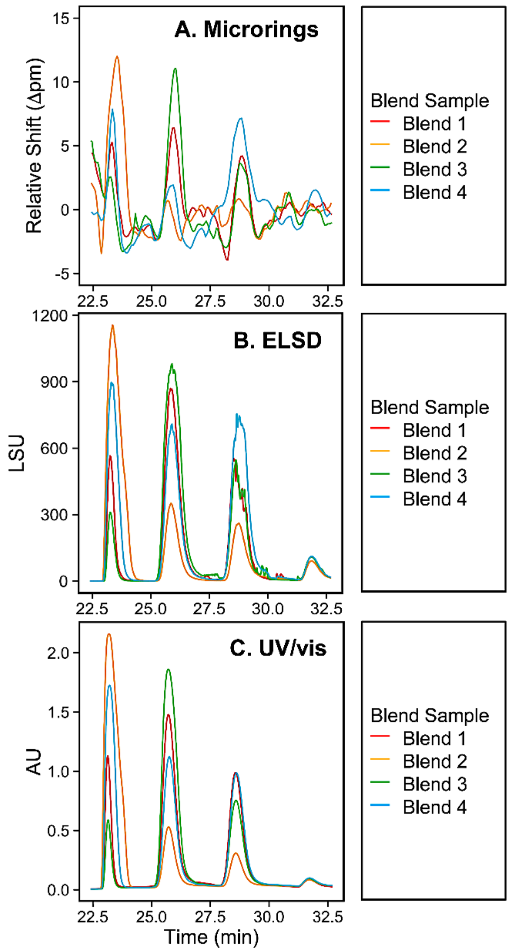

Figure 5: Copolymer blend analysis by various detectors
Polymer blends were made by mixing three PS-PMMA copolymers at various ratios all with a concentration of 11 mg/mL in chloroform. Separations were achieved based on composition using a cyclohexane:THF gradient. Chromatograms were obtained by detection with the **A.** microring resonators **B.** evaporative light scattering (ELSD) and **C.** UV/visible (UV).

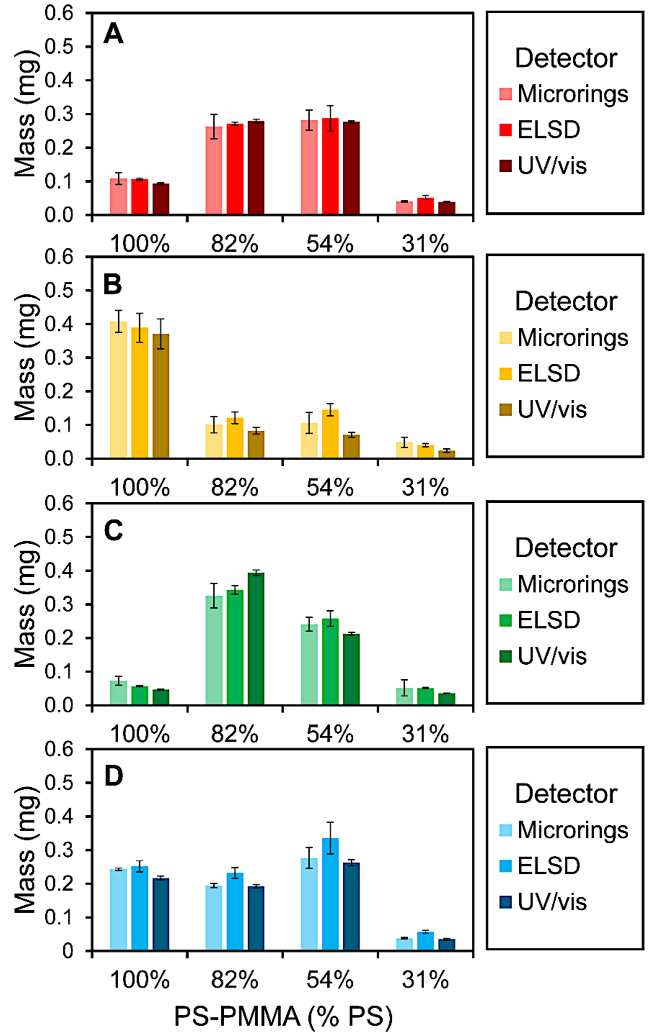

Figure 6: Quantitative Analysis of Polymer Blends
Integrating each peak area allowed for the quantification of mass detected for each component of the sample. This was done across all detectors allowing for a direct comparison, good correlation is observed since comparable mass values were obtained for each component by each method. Each histogram represents a different blend sample of the same three components A. Blend 1, B. Blend 2, C. Blend 3, and D. Blend 4.

Table 6: Polymer blend analysis, mass quantification

		Quantified Mass for Each Blend Component (mg)							
		100% PS		82% PS-PMMA		54% PS-PMMA		31% PS-PMMA	
Detector	Blend	Average	Standard Deviation	Average	Standard Deviation	Average	Standard Deviation	Average	Standard Deviation
Microrings	1	0.11	0.02	0.26	0.04	0.28	0.03	0.040	0.002
	2	0.41	0.03	0.10	0.02	0.11	0.03	0.048	0.015
	3	0.072	0.013	0.33	0.04	0.24	0.02	0.05	0.02
	4	0.24	0.003	0.19	0.006	0.28	0.03	0.038	0.002
UV	1	0.093	0.003	0.28	0.005	0.28	0.003	0.038	0.0009
	2	0.37	0.04	0.08	0.01	0.070	0.007	0.024	0.005
	3	0.047	0.0011	0.39	0.008	0.21	0.004	0.036	0.0008
	4	0.22	0.006	0.19	0.005	0.26	0.01	0.035	0.002
ELSD	1	0.11	0.003	0.27	0.005	0.29	0.04	0.052	0.006
	2	0.39	0.04	0.12	0.02	0.15	0.02	0.040	0.005
	3	0.057	0.0013	0.34	0.013	0.26	0.02	0.051	0.002
	4	0.25	0.02	0.23	0.02	0.34	0.05	0.057	0.004

The 31% PS standard was measured over a narrower mass range because of the pressure limits of the HPLC system. Injecting too much mass of the later eluting standards caused the HPLC system to go over pressure. These standards are least soluble in the initial gradient conditions, resulting in precipitation onto the column and increased pressure. The mass concentration response was investigated by plotting mass injected against the integrated peak area for each detection method allowing for mass calibrations of 4 PS-PMMA standards, as seen in Figure 4. Here all y intercepts were set to 0 as a means to normalize across detectors. Comparing these mass calibration curves demonstrates the linearity of the microring resonator response (Figure 4A). The UV detector also has a linear response for the 4 PS-PMMA standards and slope offset correlates with PS content (Figure 4B). The fitting parameters for the microring resonator and UV response curves are found in Table 3. As for the ELSD, the response is non-linear (Figure 4C) and the fitting parameters are provided in Table 4. As mentioned this non-linearity makes quantification difficult to determine mass concentrations. Calibration curve points represent the average of three replicate experiments, and error bars represent the standard deviation from visible over the plot range presented. As mentioned above, we attribute the increased error of the microring resonator platform to inherent noise of the detector and the reduced precision of baseline fitting for peak integration. Finally, limits of detection (LOD) and limits of quantification (LOQ) were calculated for each detector (Table 5). LOD and LOQ are dependent on the standard composition since detection differs slightly due to differing RI contrast for the microrings, though this changes depending on the analyte/mobile phase pairing. Therefore in cases where RI contrast is low increasing sample size can be advantageous especially in polymer separations where sample size is rarely a limitation. The LODs and LOQs for UV also depend on standard composition or more specifically chromophore content, this however is a more difficult challenge when the analyte of interest lacks such chemical signature.

Polymer Blend Separations

Polymer blends were prepared as mixtures of the various PS-PMMA copolymers at different ratios. These included varying amounts of 100%, 82%, and 54% PS with the 31% PS standard used as an internal control having constant concentration constant across all 4 synthetic blends. For blend separations a total mass of 0.75 mg was injected on the column and detection was carried out using all three detectors. Representative chromatograms for n=3 blend separations are shown in Figure 5 (peak areas presented in Figure S5), with the same elution order as in Figure 2 (highest to lowest PS). Using the compositional calibration presented in Figure 3 we can identify each individual component of the blends, the first eluted peak is 100%, second 82%, third 54% and last eluted is the 31%. The 31% component was used as an internal standard and the consistency of the sample preparation across blends is verified by looking at the overlapping 31% blend component.

Quantification and Analysis of Polymer Blend Samples

The quantification of mass injected was done using the corresponding calibration curve for each peak component. Peak components were identified by retention time. A comparison of quantification across detectors for each blend can be found in Figure 6 and Table 6, additionally actual mass are provided in Table S1. In this comparison, similar values are observed for each method, verifying the quantitative ability of the microring resonators. The microring resonator platform appears to offer some significant advantages over traditional HPLC detectors. Its large dynamic range of response enables detection of analytes on top of a strongly sloping gradient baseline. Observation of the gradient baseline (i. e., the gradient composition) itself is another advantage, which is not possible with traditional LC detectors (Figure 7). Real-time monitoring of the solvent gradient can account for fluctuations in pump performance and detection of non-ideal gradients serving as a diagnostic tool to monitor run integrity. Additionally, observation of the gradient baseline enables detection of gradient distortion which can compromise resolution. This in practice is demonstrated in Figure 7, where a 100% cyclohexane to 100% THF gradient was utilized without injections. Using the programed methods of Figure 7A the raw gradient traces in Figure 7B were transformed into relative shift (Δpm) as a function of %THF Figure 7C. Here (Figure 7C) it is observed that with a steep gradient (i.e. 8 minutes), which is equivalent to approximately 1 column volume, there is a nonlinear distortion in the raw gradient traces that is not observed in methods of multiple column volumes. The 100 min trace covers >10 column volumes and illustrates a linear gradient which is ideal for separations of better resolution. Gritti and Guiochon observed these same distortion trends using reverse phase gradients.[48] On a side note, comparing raw gradient traces of different lengths (Figure 7B) there is the observation of different gradient slopes due to varied rates of solvent mixing however the overall change in RI is consistent. Therefore, if run integrity was compromised it would be obvious early on before translating to traces into a function of solvent composition. In fact closer examination of Figure 1A, which utilizes a truncated gradient (95% (95:5 cyclohexane: THF) to 10% cyclohexane) and has a gradient length of 20 minutes, reveals a slight bit of curvature in a nominally linear gradient. This curvature may indicate that our gradient was slightly steeper than optimal, however further investigation implied that time is not a factor since the curvature was nearly the same across methods of various lengths (Figure S6).[48] Similar curvature among the various gradients does not appear to be an artifact of the method itself but is likely due to the use of 5% strong solvent in reservoir A or inadequate solvent mixing. The use of strong solvent in reservoir A was necessary to maintain complete solubility of all analytes on injection. Although its presence appears to offer an advantage in terms of gradient ideality, it limits retention of copolymers with larger % styrene. The reason for minimal gradient distortion is that THF is always present in the column so there is minimal loss of THF as the gradient begins due to interaction of THF with the column. Further, UV absorbing solvents (e. g., toluene) are compatible with microring resonator platform, meaning direct monitoring of the gradient is possible. Finally, although all detectors used in this study required calibration for mass concentration determination, the microring resonator platform is believed to have an advantage over ELSD. Although not obvious for the system studied here, the ELSD typically exhibits both a solvent and polymer composition dependence to its response,[24,49] and both of these dependencies are typically nonlinear. On the other hand, the microring resonator response is only dependent on the polymer composition eluting at a particular time in the gradient, and the response to that component is linear with concentration.

Conclusions

Commercial detectors compatible with gradient elution HPLC, such as ELSD and UV, have limitations for quantitative CCD measurements of industrially relevant polymers. Using microring resonators as gradient detectors for the separation of various PS-PMMA copolymers demonstrates advantages of the platform for complex polymer analysis. Foremost, the gradient compatibility of the microring resonator platform was exhibited, showing that refractive index based detection of gradient elution LC can be achieved unlike commercial dRI detectors. Here it was also observed that polymers like PMMA, which do not have a chromophore, can be detected by the microrings, providing an advantage over the commonly used UV detector. Additionally, various calibrations were performed for composition and mass injected, where mass calibrations illustrated the linearity of the microring resonator response. Linearity is where commonly used detectors like ELSD struggle since linearity is important for the ability to quantify mass concentrations. The quantitative results further support the applicability of the microring resonator platform for quantitative polymer analysis in solvent gradients.

However, it is important to also point out the challenges of the microring resonator platform as a solvent gradient chromatography detector. In comparison to commercial detectors, the baseline noise is larger. Because of the increased noise, there are additional processing steps for data analysis. Also, the decreased surface sensitivity with high molecular weights is another limitation. Commercial development of this platform for chromatographic separations would

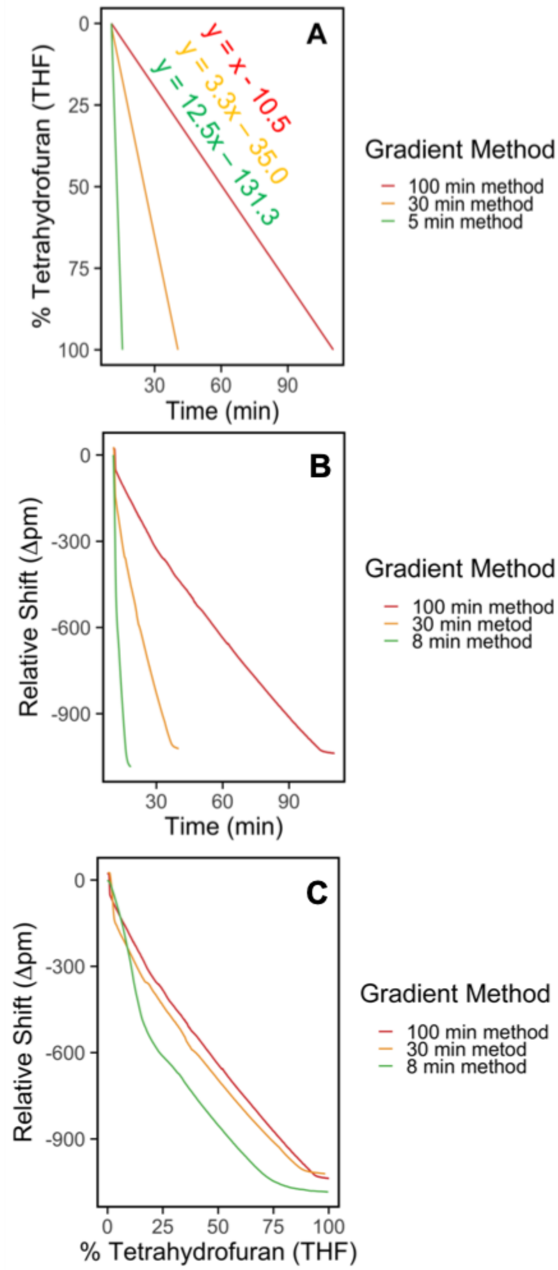

Figure 7: Real Time Monitoring of Solvent Gradient Baseline
(A) Here we wrote three gradient methods (100% cyclohexane to 100 % THF) of varying length. By plotting zoomed in traces (B) as relative shift versus time and (C) as a function of solvent composition demonstrates how gradient ideality can be directly evaluated and optimized. For example, the 8 min method (equivalent to 1 column volume) shows a non-ideal distorted trace which will limit resolution. An optimized trace is represented by the 100 min method which covers over 10 column volumes.

likely require improvements in each of those areas, which is an active area of continued research.

In summary, microring resonators offer much applicability to polymer analysis with broad versatility in a single detector. A universal linear mass concentration detector for use in solvent gradient HPLC is a longstanding challenge for separations. Despite the described limitations of the platform, this work represents an advancement toward a new detector technology for industrial copolymer analysis.

Acknowledgements

We acknowledge financial support from The Dow Chemical Company through the University Partnership Initiative Program. RCB acknowledges support from the National Science Foundation through Award 1744105.

Supplemental Information

Please find supplemental figures for interface and flow diagrams, peak integration comparisons and a table of actual polymer blend compositions.

References

(1) Hiemenz, P.; Lodge, Timothy. *Polymer Chemistry*, 2nd ed.; CRC Press.
(2) Uliyanchenko, E.; Wal, S. van der; J. Schoenmakers, P. Challenges in Polymer Analysis by Liquid Chromatography. *Polym. Chem.* **2012**, *3* (9), 2313–2335.
(3) Podzimek, S. Molar Mass Distribution by Size Exclusion Chromatography: Comparison of Multi-Angle Light Scattering and Universal Calibration. *J. Appl. Polym. Sci.* **2019**, *136*, 47561.
(4) Kou, D.; Manius, G.; Zhan, S.; Chokshi, H. P. Size Exclusion Chromatography with Corona Charged Aerosol Detector for the Analysis of Polyethylene Glycol Polymer. *J. Chromatogr. A* **2009**, *1216* (28), 5424–5428.
(5) Striegel, A. M. Multiple Detection in Size-Exclusion Chromatography of Macromolecules. *Anal. Chem.* **2005**, *77* (5), 104 A-113 A.
(6) Södergård, A.; Stolt, M. Properties of Lactic Acid Based Polymers and Their Correlation with Composition. *Prog. Polym. Sci.* **2002**, *27* (6), 1123–1163.
(7) Glöckner, G. Chemical Heterogeneity of Copolymers. In *Gradient HPLC of Copolymers and Chromatographic Cross-Fractionation*; Glöckner, G., Ed.; Springer Berlin Heidelberg: Berlin, Heidelberg, 1991; pp 14–24.
(8) Murgasova, R.; Hercules, D. M. Polymer Characterization by Combining Liquid Chromatography with MALDI and ESI Mass Spectrometry. *Anal. Bioanal. Chem.* **2002**, *373* (6), 481–489.
(9) Campbell, J. D.; Allaway, J. A.; Teymour, F.; Morbidelli, M. High-Temperature Polymerization of Styrene: Mechanism Determination with Preparative Gel Permeation Chromatography, Matrix-Assisted Laser Desorption/Ionization Time-of-Flight Mass Spectrometry, and 13C Nuclear Magnetic Resonance. *J. Appl. Polym. Sci.* **2004**, *94* (3), 890–908.
(10) Willemse, R. X. E.; Staal, B. B. P.; Donkers, E. H. D.; van Herk, A. M. Copolymer Fingerprints of Polystyrene-Block-Polyisoprene by MALDI-ToF-MS. *Macromolecules* **2004**, *37* (15), 5717–5723.
(11) Uliyanchenko, E. Applications of Hyphenated Liquid Chromatography Techniques for Polymer Analysis. *Chromatographia* **2017**, *80* (5), 731–750.
(12) Dwyer, J. L.; Zhou, M. Polymer Characterization by Combined Chromatography-Infrared Spectroscopy https://www.hindawi.com/journals/ijs/2011/694645/. vol 2011, Article ID 694645.
(13) Glöckner, G. Separation of Copolymers by Composition through Gradient High-Performance Liquid Chromatography. In *Gradient HPLC of Copolymers and Chromatographic Cross-Fractionation*; Glöckner, G., Ed.; Springer Berlin Heidelberg: Berlin, Heidelberg, 1991; pp 113–147.
(14) Gradient Elution. In *Introduction to Modern Liquid Chromatography*; John Wiley & Sons, Ltd, 2010; pp 403–473.
(15) Dixon, R. W.; Peterson, D. S. Development and Testing of a Detection Method for Liquid Chromatography Based on Aerosol Charging. *Anal. Chem.* **2002**, *74* (13), 2930–2937.
(16) Vehovec, T.; Obreza, A. Review of Operating Principle and Applications of the Charged Aerosol Detector. *J. Chromatogr. A* **2010**, *1217* (10), 1549–1556.
(17) Charlesworth, J. M. Evaporative Analyzer as a Mass Detector for Liquid Chromatography. *Anal. Chem.* **1978**, *50* (11), 1414–1420.
(18) Arndt, J. H.; Macko, T.; Brüll, R. Application of the Evaporative Light Scattering Detector to Analytical Problems in Polymer Science. *J. Chromatogr. A* **2013**, *1310* (Supplement C), 1–14.
(19) Mojsiewicz-Pieńkowska, K. Size-Exclusion Chromatography with Evaporative Light Scattering Detection: Method for Determination of Polydimethylsiloxanes. I. Testing Dependence of Molecular Weight of Polydimethylsiloxanes and Injected Mass upon the Detector Signal. *J. Chromatogr. B*

Analyt. Technol. Biomed. Life. Sci. **2008**, *865* (1–2), 1–6.
(20) Takahashi, K.; Kinugasa, S.; Senda, M.; Kimizuka, K.; Fukushima, K.; Matsumoto, T.; Shibata, Y.; Christensen, J. Quantitative Comparison of a Corona-Charged Aerosol Detector and an Evaporative Light-Scattering Detector for the Analysis of a Synthetic Polymer by Supercritical Fluid Chromatography. *J. Chromatogr. A* **2008**, *1193* (1), 151–155.
(21) Biochemical and Synthetic Polymer Separations. In *Introduction to Modern Liquid Chromatography*; John Wiley & Sons, Ltd, 2010; pp 569–663.
(22) Vervoort, N.; Daemen, D.; Török, G. Performance Evaluation of Evaporative Light Scattering Detection and Charged Aerosol Detection in Reversed Phase Liquid Chromatography. *J. Chromatogr. A* **2008**, *1189* (1), 92–100.
(23) Webster, G. K.; Jensen, J. S.; Diaz, A. R. An Investigation into Detector Limitations Using Evaporative Light-Scattering Detectors for Pharmaceutical Applications. *J. Chromatogr. Sci.* **2004**, *42* (9), 484–490.
(24) Boborodea, A.; O'Donohue, S. Linearization of Evaporative Light Scattering Detector Signal. *Int. J. Polym. Anal. Charact.* **2017**, *22* (8), 685–691.
(25) Wade, J. H.; Bailey, R. C. Applications of Optical Microcavity Resonators in Analytical Chemistry. *Annu. Rev. Anal. Chem.* **2016**, *9*, 1–25.
(26) Wade, J. H.; Bailey, R. C. Refractive Index-Based Detection of Gradient Elution Liquid Chromatography Using Chip-Integrated Microring Resonator Arrays. *Anal. Chem.* **2014**, *86* (1), 913–919.
(27) Schoenmakers, P.; Aarnoutse, P. Multi-Dimensional Separations of Polymers. *Anal. Chem.* **2014**, *86* (13), 6172–6179.
(28) Graybill, R. M.; Para, C. S.; Bailey, R. C. PCR-Free, Multiplexed Expression Profiling of MicroRNAs Using Silicon Photonic Microring Resonators. *Anal. Chem.* **2016**, *88* (21), 10347–10351.
(29) Washburn, A. L.; Shia, W. W.; Lenkeit, K. A.; Lee, S.-H.; Bailey, R. C. Multiplexed Cancer Biomarker Detection Using Chip-Integrated Silicon Photonic Sensor Arrays. *Analyst* **2016**, *141* (18), 5358–5365.
(30) Wade, J. H.; Alsop, A. T.; Vertin, N. R.; Yang, H.; Johnson, M. D.; Bailey, R. C. Rapid, Multiplexed Phosphoprotein Profiling Using Silicon Photonic Sensor Arrays. *ACS Cent. Sci.* **2015**, *1* (7), 374–382.
(31) Shopova, S. I.; White, I. M.; Sun, Y.; Zhu, H.; Fan, X.; Frye-Mason, G.; Thompson, A.; Ja, S. On-Column Micro Gas Chromatography Detection with Capillary-Based Optical Ring Resonators. *Anal. Chem.* **2008**, *80* (6), 2232–2238.
(32) Zhu, H.; White, I. M.; Suter, J. D.; Zourob, M.; Fan, X. Integrated Refractive Index Optical Ring Resonator Detector for Capillary Electrophoresis. *Anal. Chem.* **2007**, *79* (3), 930–937.
(33) Kim, D. C.; Dunn, R. C. Integrating Whispering Gallery Mode Refractive Index Sensing with Capillary Electrophoresis Separations Using Phase Sensitive Detection. *Anal. Chem.* **2016**, *88* (2), 1426–1433.
(34) Orlet, J. D.; Bailey, R. C. Silicon Photonic Microring Resonator Arrays as a Universal Detector for Capillary Electrophoresis. *Anal. Chem.* **2020**, *92* (2), 2331–2338.
(35) Ye, D.; Wang, W.; Moline, D.; Islam, M. S.; Chen, F.; Wang, P. A Microwave Flow Detector for Gradient Elution Liquid Chromatography. *Anal. Chem.* **2017**.
(36) Mordan, E.; Wade, J. H.; Wiersma, Z. S. B.; Pearce, E.; Pangburn, T. O.; deGroot, A. W.; Meunier, D. M.; Bailey, R. C. Silicon Photonic Microring Resonator Arrays for Mass Concentration Detection of Polymers in Isocratic Separations. *Anal. Chem.* **2018**. *91*, 1011-1018.
(37) Iqbal, M.; Gleeson, M. A.; Spaugh, B.; Tybor, F.; Gunn, W. G.; Hochberg, M.; Baehr-Jones, T.; Bailey, R. C.; Gunn, L. C. Label-Free Biosensor Arrays Based on Silicon Ring Resonators and High-Speed Optical Scanning Instrumentation. *IEEE J. Sel. Top. Quantum Electron.* **2010**, *16* (3), 654–661.
(38) Brun, Y.; Alden, P. Gradient Separation of Polymers at Critical Point of Adsorption. *J. Chromatogr. A* **2002**, *966* (1), 25–40.
(39) Glöckner, G. Special Features of Polymer HPLC. In *Gradient HPLC of Copolymers and Chromatographic Cross-Fractionation*; Glöckner, G., Ed.; Springer Berlin Heidelberg: Berlin, Heidelberg, 1991; pp 45–55.
(40) Mourey, T. H. Polymer Adsorption Chromatography with Evaporative Light-Scattering Detection. *J. Chromatogr. A* **1986**, *357*, 101–106.
(41) Mekap, D.; Macko, T.; Brüll, R.; Cong, R.; deGroot, W.; Parrott, A.; Yau, W. Multiple-Injection Method in High-Temperature Two-Dimensional Liquid Chromatography (2D HT-LC). *Macromol. Chem. Phys.* **2014**, *215* (4), 314–319.
(42) Mengerink, Y.; Peters, R.; Kerkhoff, M.; Hellenbrand, J.; Omloo, H.; Andrien, J.; Vestjens, M.; van der Wal, S. Analysis of Linear and Cyclic Oligomers in Polyamide-6 without Sample Preparation by Liquid Chromatography Using the Sandwich Injection Method: II. Methods of Detection and Quantification and Overall Long-Term Performance. *J. Chromatogr. A* **2000**, *878* (1), 45–55.

(43) Jiang, X.; van der Horst, A.; Schoenmakers, P. J. Breakthrough of Polymers in Interactive Liquid Chromatography. *J. Chromatogr. A* **2002**, *982* (1), 55–68.
(44) Cleveland, W. S.; Devlin, S. J. Locally Weighted Regression: An Approach to Regression Analysis by Local Fitting. *J. Am. Stat. Assoc.* **1988**, *83* (403), 596–610.
(45) Smart, C.; Willis, E. Determination of Refractive Indices of Polystyrene Latices by Light Scattering. *J. Colloid Interface Sci.* **1967**, *25* (4), 577–583.
(46) Beadie, G.; Brindza, M.; Flynn, R. A.; Rosenberg, A.; Shirk, J. S. Refractive Index Measurements of Poly(Methyl Methacrylate) (PMMA) *Appl. Opt.* **2015**, *54* (31), F139–F143.
(47) Luchansky, M. S.; Washburn, A. L.; Martin, T. A.; Iqbal, M.; Gunn, L. C.; Bailey, R. C. Characterization of the Evanescent Field Profile and Bound Mass Sensitivity of a Label-Free Silicon Photonic Microring Resonator Biosensing Platform. *Biosens. Bioelectron.* **2010**, *26* (4), 1283–1291.
(48) Gritti, F.; Guiochon, G. Separations by Gradient Elution: Why Are Steep Gradient Profiles Distorted and What Is Their Impact on Resolution in Reversed-Phase Liquid Chromatography. *J. Chromatogr. A* **2014**, *1344*, 66–75.
(49) Mourey, T. H.; Oppenheimer, L. E. Principles of Operation of an Evaporative Light-Scattering Detector for Liquid Chromatography. *Anal. Chem.* **1984**, *56* (13), 2427–2434.

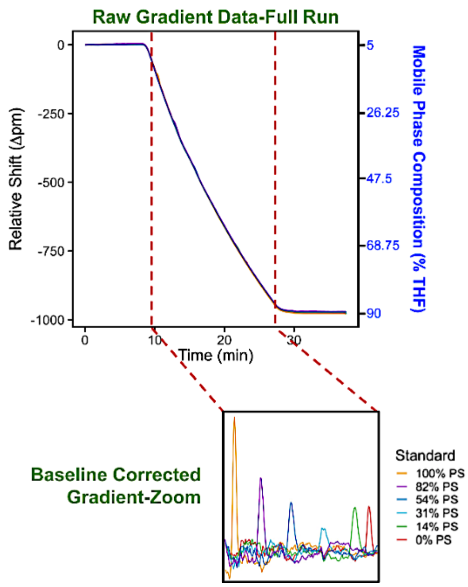
Raw Gradient Data-Full Run
Relative Shift (Δpm)
0
-250
-500
-750
-1000
0
10
20
30
Time (min)
5
26.25
47.5
68.75
90
Mobile Phase Composition (% THF)
Baseline Corrected Gradient-Zoom
Standard
100% PS
82% PS
54% PS
31% PS
14% PS
0% PS